Vol 15 No 2, February 2006
1009-1963/2006/15(02)/0375-08

Chinese Physics

© 2006 Chin. Phys. Soc.
and IOP Publishing Ltd

Theory of two-photon micromaser: competition among different transition processes*

Sun Wei-Hui(孙为辉)[a)b)], Du Si-De(杜四德)[a)†], and Chen Xiao-Shuang(陈效双)[c)]

[a)] *Department of Physics, Fudan University, Shanghai 200433, China*
[b)] *Surface Physics Laboratory (National Key Laboratory), Fudan University, Shanghai 200433, China*
[c)] *National Laboratory for Infrared Physics, Shanghai Institute of Technical Physics, Chinese Academy of Sciences, 500 Yu-Tian Road, Shanghai 200083, China*

(Received 11 May 2005; revised manuscript received 26 October 2005)

We have investigated the steady-state cavity-field properties of a single-mode two-photon micromaser when the atoms in a cascade three-level configuration are initially prepared in a mixture of the upper and intermediate states. The mean photon number, trapping state and sub-Poissonian effect are discussed with upper (intermediate)-state population changing from 1(0) to 0(1). These properties are very different from those in a pure two- or one-photon transition process, due to the competition among different transition processes. In particular, the trapping states of nonzero photons are discovered in this system under some conditions, which is contrary to the previous findings.

Keywords: two-photon micromaser, trapping states, sub-Poissonian distribution
PACC: 4250, 4252, 3280

1. Introduction

Cavity quantum electrodynamics(QED) has been widely studied in recent years,[1−4] because it can be used to experimentally test fundamental problems in quantum mechanics. The basic core in the study of cavity QED is Jaynes–Cummings model.[5] A fundamental part in this framework is a one-atom maser or micromaser. Recently a two-photon micromaser has attracted many scientists' interest,[6−10] since the two-photon process emits photons in pairs simultaneously, it may lead to some interesting phenomena different from those appearing in a one-photon process. A few years ago, a two-photon micromaser was operated,[6] which offers us an opportunity to study the interaction between atoms and a single mode of electromagnetic field. The theory of the two-photon micromaser was initiated by Brune *et at*[7] and Davidovich *et al*,[8] then developed by Zubairy *et al.*[9,10] It is discovered in Ref.[9] that there are no other trapping states except the vacuum states, which is different from the one-photon micromaser.[11] In this paper we investigate photon statistics of a two-photon micromaser when the atoms are initially prepared in a mixture of the upper and intermediate states. Under atomic initial conditions, there exist various transition processes: two-photon emission(an upper state → an intermediate state → a lower state), one-photon emission (an intermediate state → a lower state), and one-photon absorption (an intermediate state → an upper state). It is the competition among these transition processes that influences the properties of the cavity field. Here our purpose is just to investigate how this competition affects the intensity, trapping states and sub-Poissonian properties of the cavity field on assumption that there exist small detunings between the intermediate state and cavity field. Such atomic level configurations are experimentally available.[6]

In this paper, to start with, we make use of time-evolution operator with two different coupling constants to calculate the reduced density operator of the cavity field. Then we investigate the trapping states in a two-photon micromaser. We obtain four kinds of trapping states besides vacuum states[9] in the in-

*Project supported by the National Natural Science Foundation of China, the National Key Basic Research Special Foundation of China, the Major Program of the National Natural Science Foundation of China (Grant No 10234040), and the Shanghai Foundation for Development of Science and Technology (Grant No 02DJ14066).

†E-mail: sddu@fudan.ac.cn

termediate states of the excited atoms. Finally, we investigate the photon statistics in the two-photon micromaser by changing the initial states of the excited atoms in the presence of thermal photons $\overline{n}_b = 0.1$.

The above content is organized as follows. In Section 2, we derive a master equation of cavity fields and present the steady-state photon-number distributions. In Section 3, based on the steady-state photon-number distributions, we numerically investigate the trapping states in the two-photon micromaser besides the vacuum trapping states. In Section 4, we further study the features of the photon statistics when $\overline{n}_b = 0.1$ under different conditions. Our main results are summarized in Section 5.

2. Model and theory

Consider a beam consisting of three-level atoms in a cascade configuration (see Fig.1), which is injected into a single-mode quantized cavity field. The exact two-photon resonance is assumed to happen between the upper state $|a\rangle$ and lower state $|c\rangle$ so that the intermediate state $|b\rangle$ is detuned from the exact one-photon resonance, with a detuning defined by

$$\Delta = \omega - (\omega_a - \omega_b) = (\omega_b - \omega_c) - \omega, \tag{1}$$

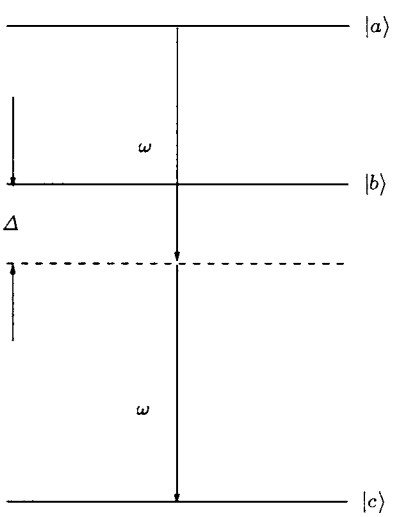


Fig.1. Atomic level configuration used throughout this paper.

where ω is the frequency of the resonant mode of the micromaser cavity. The frequencies associated with the atomic levels $|a\rangle$, $|b\rangle$, and $|c\rangle$ are ω_a, ω_b, and ω_c, respectively. The Hamiltonian in the interaction picture can be expressed as

$$\begin{aligned} V_{\rm I} =& \hbar g_1(a|a\rangle\langle b|{\rm e}^{-{\rm i}\Delta t} + a^+|b\rangle\langle a|{\rm e}^{{\rm i}\Delta t}) \\ &+ \hbar g_2(a|b\rangle\langle c|{\rm e}^{{\rm i}\Delta t} + a^+|c\rangle\langle b|{\rm e}^{-{\rm i}\Delta t}), \end{aligned} \tag{2}$$

where g_1 and g_2 are the coupling constants for the transitions $a \to b$ and $b \to c$, respectively. As a result, the temporal evolution operator U can be theoretically acquired in this interaction picture, which is given by ${\rm i}\hbar {\rm d}U/{\rm d}t = V_I U$. Through tedious mathematical calculations, one can obtain the following expression:

$$U = \begin{pmatrix} 1 - aG_{11}a^+ & -{\rm i}g_1 aQ & -aG_{12}a \\ -{\rm i}g_1 Q^+ a^+ & O^+ & -{\rm i}g_2 Q^+ a \\ -a^+ G_{21}a^+ & -{\rm i}g_2 a^+ Q & 1 - a^+ G_{22}a \end{pmatrix}, \tag{3}$$

where

$$\widetilde{\Lambda}_{11} = \frac{g_1^2}{(g_1^2 a^+ a + g_2^2 a a^+)}, \tag{4}$$

$$\widetilde{\Lambda}_{22} = \frac{g_2^2}{(g_1^2 a^+ a + g_2^2 a a^+)}, \tag{5}$$

$$\widetilde{\Lambda}_{21} = \widetilde{\Lambda}_{12} = \frac{g_1 g_2}{(g_1^2 a^+ a + g_2^2 a a^+)}, \tag{6}$$

$$\Lambda = g_1^2 a^+ a + g_2^2 a a^+ + \Delta^2/4, \tag{7}$$

$$O = (\cos\sqrt{\Lambda}t + ({\rm i}\Delta \sin\sqrt{\Lambda}t/2\sqrt{\Lambda}))e^{-{\rm i}\Delta t/2}, \tag{8}$$

$$Q = \sin\sqrt{\Lambda}t e^{-{\rm i}\Delta t/2}/\sqrt{\Lambda}, \tag{9}$$

$$G_{11} = \widetilde{\Lambda}_{11}(1 - O), \tag{10}$$

$$G_{12} = \widetilde{\Lambda}_{12}(1 - O), \tag{11}$$

$$G_{21} = \widetilde{\Lambda}_{21}(1 - O), \tag{12}$$

$$G_{22} = \widetilde{\Lambda}_{22}(1 - O). \tag{13}$$

Assume $g_1 = g_2$, then Eq.(3) will be slightly different from the temporal evolution operator U given in Ref.[12]. If we apply the same initial condition as that in Ref.[9], we can obtain the results similar to those in Ref.[9]. So the results in Ref.[12] may have a few flaws.

Now we apply these results to calculating the photon-number distribution in the two-photon micromaser. The excited atoms are assumed to be initially in a mixture state of $|a\rangle$ and $|b\rangle$ with the probabilities of ρ_{aa} and ρ_{bb} (of course, $\rho_{aa} + \rho_{bb} = 1$), respectively. Such states can be achieved experimentally, for example, in Ref.[13]. When such atoms are injected into the cavity at the time $t_0 = 0$, the total density operator for the atom–field system can be expressed as

$$\begin{aligned} \rho_T(t_0 = 0) =& \rho_f \otimes \rho_A \\ =& (\rho_{aa}|a\rangle\langle a| + \rho_{bb}|b\rangle\langle b|) \\ & \otimes \sum_{\psi} P_\psi |\psi\rangle\langle\psi| \\ =& \rho_{aa} \sum_{k,l} |a,k\rangle \rho_{kl}(0) \langle l,a| \\ & + \rho_{bb} \sum_{k,l} |b,k\rangle \rho_{kl}(0) \langle l,b|. \end{aligned} \tag{14}$$

After the atoms pass through the cavity, one can obtain the total density operator at that time

$$\rho_{\rm T}(\tau) = U(\tau)\rho_{\rm T}(0)U^{+}(\tau). \tag{15}$$

If $U(\tau)$ acts on the state $|a,k\rangle$ directly, we obtain

$$U(\tau)|a,k\rangle = \begin{pmatrix} \left[\frac{g_1^2(n+1)}{\beta_k\alpha_k^2}\left(\beta_k\cos\beta_k\tau + \frac{\mathrm{i}\Delta}{2}\sin\beta_k\tau - \beta_k \mathrm{e}^{\frac{\mathrm{i}\Delta\tau}{2}}\right)\mathrm{e}^{-\frac{\mathrm{i}\Delta\tau}{2}} + 1\right]|k\rangle \\ -\frac{\mathrm{i}g_1\sqrt{k+1}}{\beta_k}\mathrm{e}^{\frac{\mathrm{i}\Delta\tau}{2}}\sin\beta_k\tau|k+1\rangle \\ \frac{g_1g_2\sqrt{(k+1)(k+2)}}{\beta_k\alpha_k^2}\left(\beta_k\cos\beta_k\tau + \frac{\mathrm{i}\Delta}{2}\sin\beta_k\tau - \beta_k\mathrm{e}^{\frac{\mathrm{i}\Delta\tau}{2}}\right)\mathrm{e}^{-\frac{\mathrm{i}\Delta\tau}{2}}|k+2\rangle \end{pmatrix} = \begin{pmatrix} A_k|k\rangle \\ B_k|k+1\rangle \\ C_k|k+2\rangle \end{pmatrix}. \tag{16}$$

While $U(\tau)$ acts on the state $|b,k\rangle$, we can acquire

$$U(\tau)|b,k\rangle = \begin{pmatrix} -\mathrm{i}g_1\sqrt{k}\frac{\sin\beta_k\tau}{\beta_k}\mathrm{e}^{-\frac{\mathrm{i}\Delta\tau}{2}}|k-1\rangle \\ \left(\cos\beta_k\tau - \frac{\mathrm{i}\Delta}{2\beta_k}\sin\beta_k\tau\right)\mathrm{e}^{\frac{\mathrm{i}\Delta\tau}{2}}|k\rangle \\ \frac{-\mathrm{i}g_2\sqrt{k+1}\sin\beta_k\tau}{\beta_k}\mathrm{e}^{-\frac{\mathrm{i}\Delta\tau}{2}}|k+1\rangle \end{pmatrix} = \begin{pmatrix} D_k|k\rangle \\ E_k|k+1\rangle \\ F_k|k+2\rangle \end{pmatrix}. \tag{17}$$

In order to obtain the field density operator, we should trace over the total density with respect to the atomic variable as follows:

$$\rho(\tau) = \mathrm{Tr}_{\rm atom}(\rho_{\rm T}(\tau)). \tag{18}$$

Assuming that the injection of each atom is at intervals of Δt, thus the injection rate is $1/\Delta t$. The change rate of the field density operator can be written as

$$\dot{\rho}_{kl} \simeq \frac{\rho_{kl}(\tau) - \rho_{kl}(0)}{\Delta t} = r_a\delta\rho_{kl}. \tag{19}$$

By applying Eq.(16) and Eq.(17) to Eq.(15), and using Eq.(18), then adding the cavity-loss terms in the standard way, we can obtain

$$\begin{aligned} r_a\delta\rho_{kl} =& H_{kl}\rho_{kl} + I_{k-1,l-1}\rho_{k-1,l-1} \\ &+ J_{k-2,l-2}\rho_{k-2,l-2} \\ &+ K_{k+1,l+1}\rho_{k+1,l+1}, \end{aligned} \tag{20}$$

where

$$\begin{aligned} H_{kl} =& r_a(\rho_{aa}A_kA_L^* + \rho_{bb}E_kE_l^* - 1) \\ &- \gamma\frac{2\overline{n}_b(k+l+1)+k+l}{2}, \end{aligned} \tag{21}$$

$$\begin{aligned} I_{kl} =& r_a(\rho_{aa}B_kB_l^* + \rho_{bb}F_kF_l^*) \\ &+ \gamma\overline{n}_b\sqrt{(l+1)(k+1)}, \end{aligned} \tag{22}$$

$$J_{kl} = r_a\rho_{aa}C_kC_l^*, \tag{23}$$

$$K_{kl} = r_a\rho_{bb}D_kD_l^* + \gamma(\overline{n}_b+1)\sqrt{kl}. \tag{24}$$

We set $k = l = n$ to derive the field photon-number distribution. At the steady state, $\dot{\rho}_{kl} = 0$. By defining $\rho_{nn} = P(n)$, Eq.(20) can be simplified as

$$\begin{aligned} &H_nP(n) + I_{n-1}P(n-1) \\ &+ K_{n+1}P(n+1) + J_{n-2}P(n-2) = 0. \end{aligned} \tag{25}$$

It is well known that $H_n + I_n + K_n + J_n = 0$. Thus it is not difficult to obtain the following result which is similar to that in Ref.[9]:

$$P(n) = P(0) \prod_{r=1}^{n} \frac{1}{K_r} \left(I_{r-1} + J_{r-1} + \cfrac{J_{r-2}K_{r-1}}{I_{r-2} + J_{r-2} + \cfrac{J_{r-3}K_{r-2}}{\ddots \cfrac{}{I_1 + J_1 + \cfrac{J_0 K_1}{I_0 + J_0}}}} \right). \tag{26}$$

In the following, based on Eq.(26), we numerically investigate the trapping states and the photon statistics by calculating the relevant averages. We define the average photon number and the normalized standard deviation as follows:

$$\langle n \rangle = \sum_{n=0}^{\infty} n P_n, \qquad \langle n^2 \rangle = \sum_{n=0}^{\infty} n^2 P_n, \tag{27}$$

$$\sigma = [\langle n^2 \rangle - \langle n \rangle^2 - \langle n \rangle] / \langle n \rangle. \tag{28}$$

For $\sigma = 0$, the field is Poissonian; for $\sigma > 0$, the field is super-Poissonian; for $\sigma < 0$, however, the field is sub-Poissonian and nonclassical. The photon noises are enhanced for $\sigma > 0$, while reduced for $\sigma < 0$. We also follow the usual practice to introduce a measure of the pumping rate normalized to the cavity decay rate $N_{\rm ex}$,

$$N_{\rm ex} = r_a / \gamma. \tag{29}$$

For simplicity, we assume $g_1 = g_2 = g$ in the following sections.

3. Trapping states

As we know, the trapping state is one of the main quantum features for micromasers,[14,15] which cannot be explained from the viewpoint of the classical field theory. These states have been long studied theoretically and led to a proposal for Fock states generation.[16] Recently, the trapping states and even pure number photon states have been realized in micromasers.[17,18] Though the trapping states have become a hot issue in the quantum optics field, only vacuum trapping states are discovered in two-photon micromasers.[9] In this section, we discuss the other kinds of trapping states in the two-photon micromasers under different conditions. Considering the existing experiments,[17,18] we set $N_{\rm ex} = 10$ and $\bar{n}_b = 0.0001$.

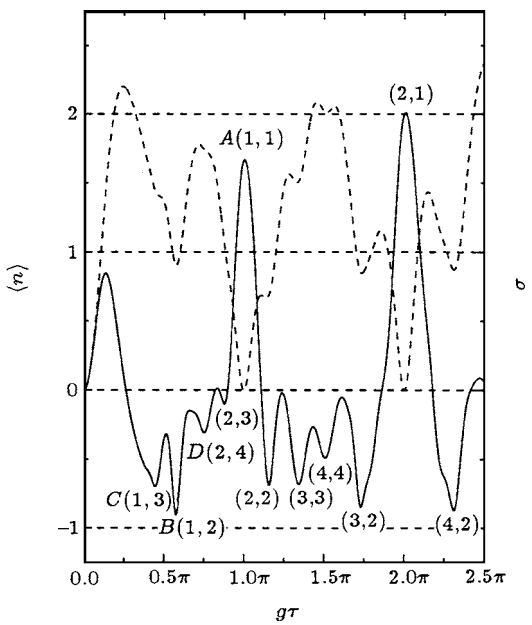


Fig.2. The mean photon number $\langle n \rangle$ (dashed line) and the normalized standard deviation of the photon numbers (solid line) σ as a function of the interaction time $g\tau$ when $\rho_{bb} = 1$, $\Delta = 0$, $N_{\rm ex} = 10$ and $n_b = 0.0001$.

If the atoms injected into the cavity are all in upper states, only vacuum trapping states appear in the cavity.[9] When we change the states of the excited atoms, however, the other trapping states will come out. Especially when the excited atoms are all in an intermediate state, four kinds of trapping states can be acquired. As shown in Fig.2, when the normalized standard deviation of the photon numbers σ arrives at some sharp minimum values, the trapping states appear correspondingly besides the vacuum trapping states which come out only when σ reaches its corresponding maximum values. The trapping states are labelled with $(k, n+1)$, which take place when the interaction time obeys the following relation:

$$g\tau_k = \frac{k\pi}{\sqrt{2n+1}}, \tag{30}$$

where k is an integer, n is the photon number of the trapping states. For example, if we want to acquire

one-photon trapping states, we can modulate the interaction time such as

$$g\tau_k = \frac{\pi}{\sqrt{3}}, \frac{2\pi}{\sqrt{3}}, \cdots . \tag{31}$$

In a particular interaction time satisfying Eq.(30), the atoms in the intermediate state $|b\rangle$ interacting with the cavity-field state $|n\rangle$ involve integer Rabi oscillations and cannot emit photons. Considering one photon loss, the cavity-field state changes from $|n\rangle$ to $|n-1\rangle$. The atoms in the intermediate state $|b\rangle$ cannot emit two photons simultaneously to help the cavity-field state to transit from $|n-1\rangle$ to $|n+1\rangle$, which is very different from what the atoms in the upper state $|a\rangle$ do. Thus it turns out that the cavity field has more trapping states when the cavity is pumped by the atoms in the intermediate state $|b\rangle$ than by the atoms in the upper state $|a\rangle$.

In Fig.3, we display the photon-number distribution for four kinds of trapping states which are indicated in Fig.2 as A, B, C, and D. In these states, the distributions are truncated at the photon numbers being 1, 2, 3, and 4, respectively, and the performances of the trapping states are very clear.

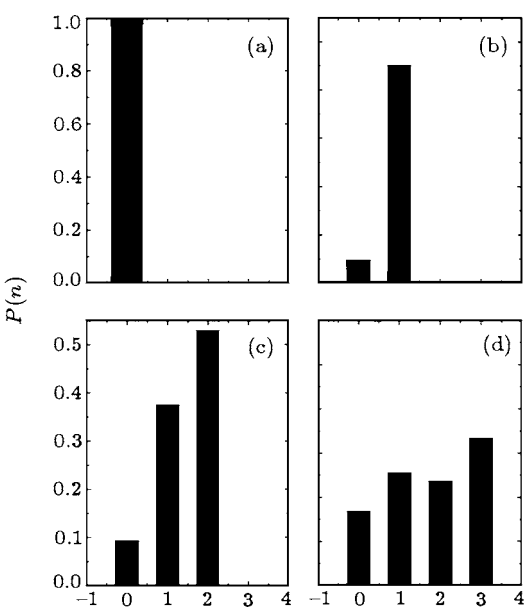


Fig.3. The photon-number distributions corresponding to the times (a), (b), (c), and (d) indicated in Fig.2, show the trapping states undoubtedly. (a), (b), (c), and (d) denote the cases of trapping zero photon, one photon, two photons, and three photons respectively in the cavity..

It should be noted that the trapping states still exist when the detunings appear in the system. We add a small detuning $\Delta = 5g$ to this system and keep the other parameters unchanged. As presented in Fig.4, the sharp minimum values A, B, C, and D denote the relevant trapping states. It is very obvious from Fig.5 that we can still acquire the one-photon trapping states. Compared with Fig.3(b), there exists a remarkably enhanced probability in the component state $|0\rangle$ of these states. Such trapping states can apply to the quantum computing and the quantum communication in the future. So we can modulate the probabilities of the states $|0\rangle$ and $|1\rangle$ by adjusting the detuning of the system.

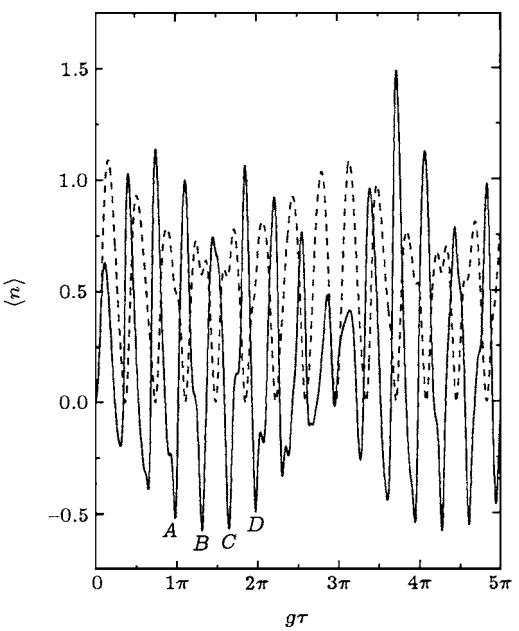


Fig.4. The mean photon number $\langle n\rangle$ (dashed line) and the normalized standard deviation of the photon numbers (solid line) σ as a function of the interaction time $g\tau$ when $\rho_{bb} = 1$, $\Delta = 5g$, $N_{\rm ex} = 10$, and $n_b = 0.0001$.

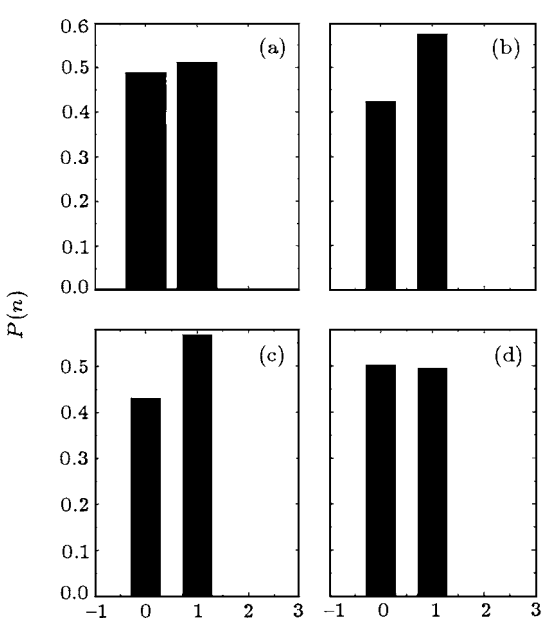


Fig.5. The photon-number distributions for the trapping states (a), (b), (c), and (d) indicated in Fig.4.

4. Features of photon statistics

In this section, we discuss how the photon statistics evolves with upper (intermediate)-state population changing from 1(0) to 0(1). In the following, we assume $N_{\rm ex} = 100$ and $\bar{n}_b = 0.1$.

4.1. The $\Delta = 0$ case

As ρ_{aa} decreases from 1 to 0, the light intensity becomes smaller and smaller, as shown in Fig.6(a). However, that is not surprising because the atom in an upper state can emit two photons, while the atom in an intermediate state can emit only one photon. As the curve E shows in Fig.6(a), when $\rho_{aa} = 0$ the light intensity (< 10) is much weaker than that (100) in the pure one-photon process or two-level system under the same conditions. In this case, all the excited atoms are in the intermediate state $|b\rangle$. When the atom transits to the lower state $|c\rangle$, one photon is emitted; otherwise when it transits to the upper state $|a\rangle$, one photon is absorbed. When the excited atoms pass through the cavity, the two processes take place simultaneously, and the final photons in the cavity are dependent on the competition between these two processes.

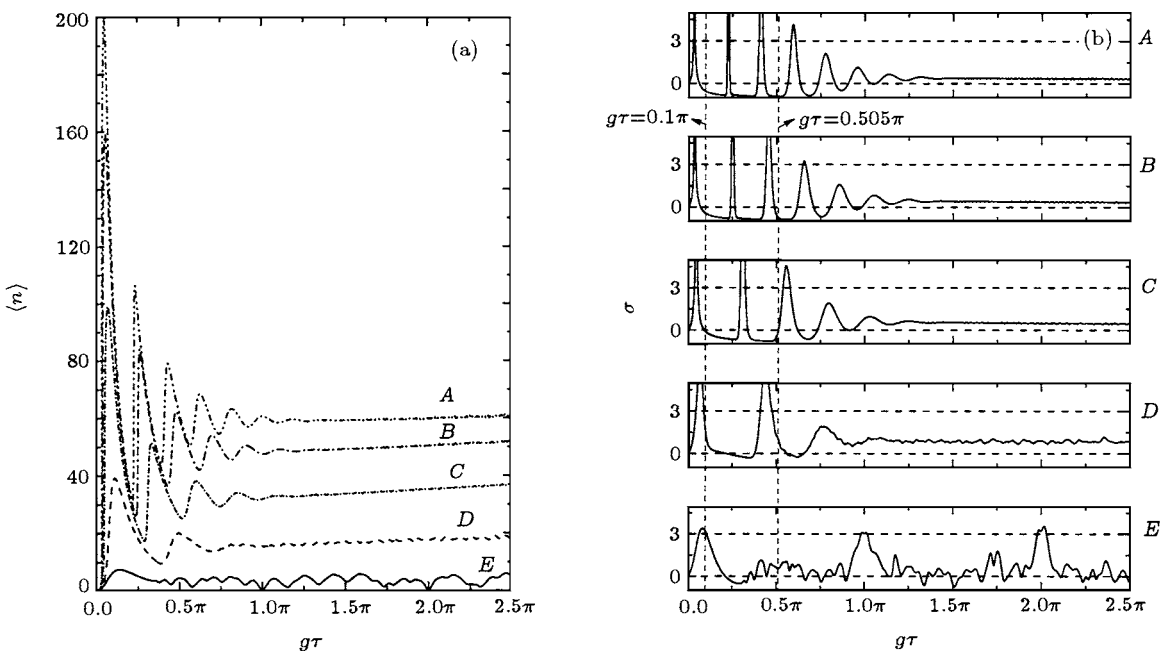


Fig.6. The mean photon number $\langle n \rangle$ (a) and the normalized standard deviation of the photon numbers σ (b) separately as a function of the interaction time $g\tau$ for different values of ρ_{aa}. A, B, C, D, and E denote the cases of $\rho_{aa} = 1.0$, 0.8, 0.5, 0.2, and 0, respectively. The other parameters are $N_{\rm ex} = 100$, $n_b = 0.1$, and $\Delta = 0$.

Figure 6(b) displays the standard deviation of photon numbers when ρ_{aa} decreases from 1 to 0. From the curve A to the curve D, the sub-Poissonian becomes weaker and weaker. However, when $\rho_{bb} = 1$ ($\rho_{aa} = 0$), the sub-Poissonian becomes stronger and appears throughout the interaction as the curve E shows. It should be noted that the strongest sub-Poissonian exists in the $\rho_{aa} = 1$ case. Therefore, the atomic mixture is not favourable to the sub-Poissonian effect, because the atoms in this state emit two kinds of incoherent photons.

Figure 7 exhibits the photon number distributions (PNDs) $P(n)$ corresponding to the fixed interaction times indicated in Fig.6(b). Figure 7 shows that the peak of $P(n)$ moves to the left side on the n-coordinate with ρ_{aa} decreasing, which shows that the average photon number decreases correspondingly. In general, the average photon number is larger at $g\tau = 0.1\pi$ than at $g\tau = 0.505\pi$. For $\rho_{aa} \geq 0.5$, the PNDs are sub-Poissonian with a single-peaked structure, and the PNDs are much narrower at $g\tau = 0.505\pi$ than at $g\tau = 0.1\pi$. For $\rho_{aa} = 0$ and 0.2, the PNDs are super-Poissonian, with a single-peaked structure at $g\tau = 0.1\pi$, but with a double-peaked structure at $g\tau = 0.505\pi$.

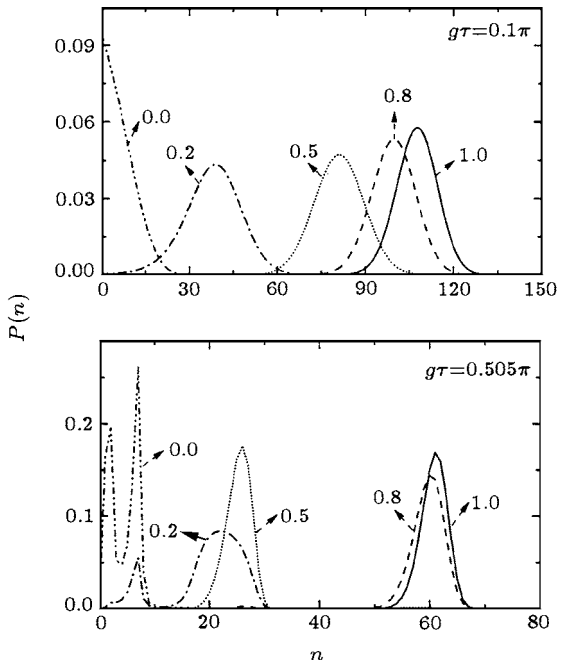


Fig.7. Steady-state photon number distributions corresponding to the points indicated in Figs.6(b). The relevant parameters are the same as those in Fig.6.

4.2. The $\Delta = 5g$ case

If we add a little detuning to this system, the average photon number, the sub-Poissonian effect and the photon number distribution will be changed. As shown in Fig.8(a), the maximum light intensity is suppressed compared to the resonance case. All curves but for the curve E oscillate with larger amplitudes and almost the same longer periods throughout the interaction, which is very different from that in Fig.6(a). It is very obvious from Fig.8(b) that the detuning is unfavourable to the sub-Poissonian effect. To illuminate the influence introduced by the detuning, we select two times indicated in Fig.8(b) the same as those in Fig.6(b) to indicate the change of the photon distribution. In the short interaction time $g\tau = 0.1\pi$, the photon distributions do not change much. In a little longer interaction time $g\tau = 0.505\pi$, however, a considerable change takes place in the cases of $\rho_{aa} = 0$ and 0.2, as shown in Fig.9. As to $\rho_{aa} = 0$, only one peak appears in the detuning system; meanwhile for $\rho_{aa} = 0.2$, the PND has a high peak and a much lower side peak. For the cases of $\rho_{aa} \geq 0.5$, the PNDs are still sub-Poissonian, but they move toward the large-n direction and are broadened.

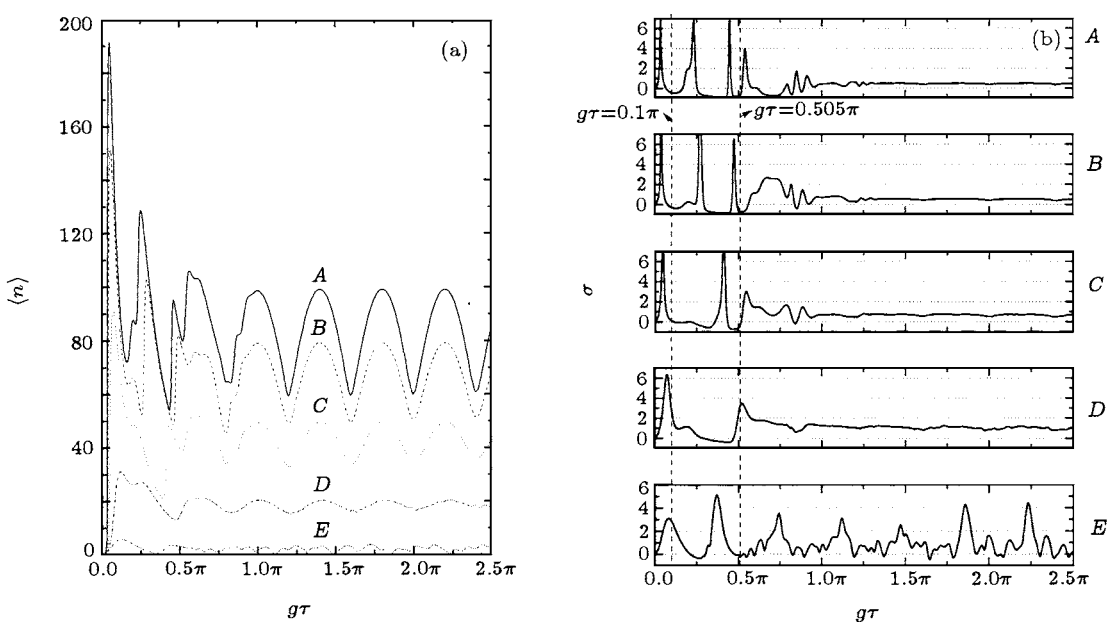


Fig.8. The mean photon number $\langle n \rangle$ (a) and the normalized standard deviation of the photon numbers σ (b) as a function of the interaction time $g\tau$ for different values of ρ_{aa}. A, B C, D, and E denote the cases of $\rho_{aa} = 1.0$, 0.8, 0.5, 0.2, and 0, respectively. The other parameters are $N_{\rm ex} = 100$, $n_b = 0.1$, and $\Delta = 5g$.

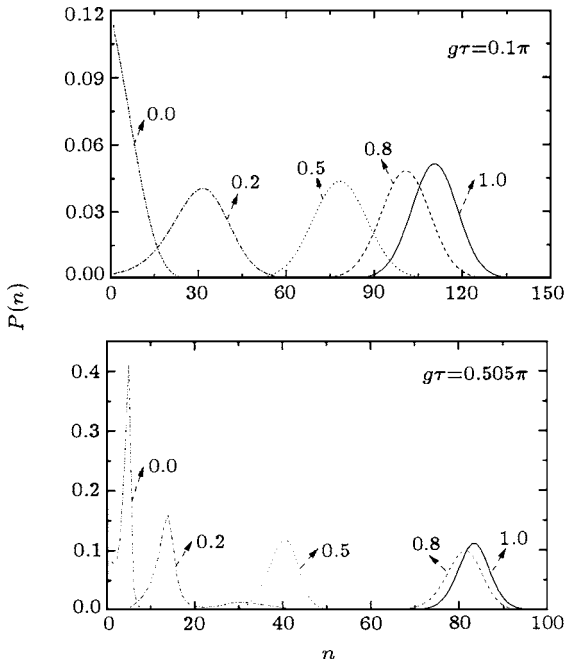


Fig.9. Steady-state photon number distributions corresponding to the points indicated in Figs.8(b).

5. Conclusion

We have investigated the steady-state cavity-field properties of a single-mode two-photon micromaser when the atoms in a cascade three-level configuration are initially prepared in a mixture of the upper and intermediate states. The trapping states of nonzero photons have been discovered in this system under some conditions. The mean photon number, trapping state and sub-Poissonian effect in both the resonance and detuning cases are discussed with upper(intermediate)-state population changing from 1(0) to 0(1). These properties are very different from those in a pure two- or one-photon transition process, due to the competition among different transition processes.

References

[1] Li F L 1996 *Acta Phys. Sin.* **45** 563 (in Chinese)

[2] Liang W Q, Chu K Q, Zhang Z M and Xie S W 2001 *Acta Phys. Sin.* **50** 2345 (in Chinese)

[3] Chen A X, Wu S D, Jin L X and Zhang Z M 2003 *Acta Phys. Sin.* **52** 2466 (in Chinese)

[4] Wu S D, Zhan Z M and Jin L X 2002 *Chin. Phys.* **11** 1272

[5] Jaynes E T and Cummings F W 1963 *Proc. IEEE.* **51** 89

[6] Brune M, Raimond J M, Goy P, Davidovich L and Haroche S 1987 *Phys. Rev. Lett.* **59** 1899

[7] Brune M, Raimond J M and Haroche S 1987 *Phys. Rev.* A **35** 154

[8] Davidovich L, Raimond J M, Brune M and Haroche S 1987 *Phys. Rev.* A **36** 3771

[9] Imrana Ashraf, Gea-Banacloche J and Zubairy M S 1990 *Phys. Rev.* A **42** 6704

[10] Toor A H, Zhu S Y and Zubairy M S 1996 *Phys. Rev.* A **53** 3529

[11] Meystre P, Rempe G and Walther H 1988 *Opt. Lett.* **13** 1078

[12] Orszag M and Retamal J C 1990 *Opt. Comm.* **79** 455

[13] Niu Y Q and Gong S Q 2004 *J. Phys. Soc. of Jap.* **73** 2131

[14] Filipowicz P, Javanainen J and Meystre P 1986 *Phys. Rev.* A **34** 3077

[15] Meschede D, Walther H and Muller G 1985 *Phys. Rev. Lett.* **54** 551

[16] Filipowicz P, Javanainen J and Meystre P 1986 *J. Opt. Soc. Am.* B **3** 906
Meystre P, Rempe G and Walther H 1988 *Opt. Lett.* B **13** 1078

[17] Weidinger M, Varcoe B T H, Heerlein R and Walther H 1999 *Phys. Rev. Lett.* **82** 3795

[18] Varcoe B T H, Brattke S, Weidinger M and Walther H 2000 *Nature* **403** 743